A Kinetically Trapped Two-Component Self Assembled Adlayer

Abdolreza Jahanbekam, Bhaskar Chilukuri, Ursula Mazur, and K W Hipps[*]

Department of Chemistry and Materials Science and Engineering Program, Washington State University, Pullman, WA 99164-4630


* To whom correspondence should be addressed:
    E-mail: hipps@wsu.edu
   Telephone: (509) 335-3033

1-Phenyloctane purification procedure: As it explained before by Bhattarai and coworkers[1] UV−Vis spectra of solutions of CoOEP in undistilled phenyloctane had two Soret bands at 392 and 420 nm instead of a single expected 392 nm band. To eliminate impurity that is complexing with CoOEP, phenyloctane was distilled over Al_2O_3 (90% Al_2O_3, 9% H_2O; Alfa products). After several distillations, the UV−Vis spectra of CoOEP in the phenyloctane showed the elimination of the band at 420 nm.

Surface structures at different relative molar ratios of coronene:CoOEP on Au(111): Figure S1 shows the STM images at different relative molar ratio of supernatant coronene:CoOEP solution. Basically we have five different STM images based on different surface structures on the surface: (a) Only CoOEP structure on the surface, (b) Coexistence of CoOEP and 1-1 structure on the surface, (c) Only 1-1 structure on the surface, (d) Coexistence of 1-1 structure and coronene structure on the surface and (e) only coronene structure on the surface.
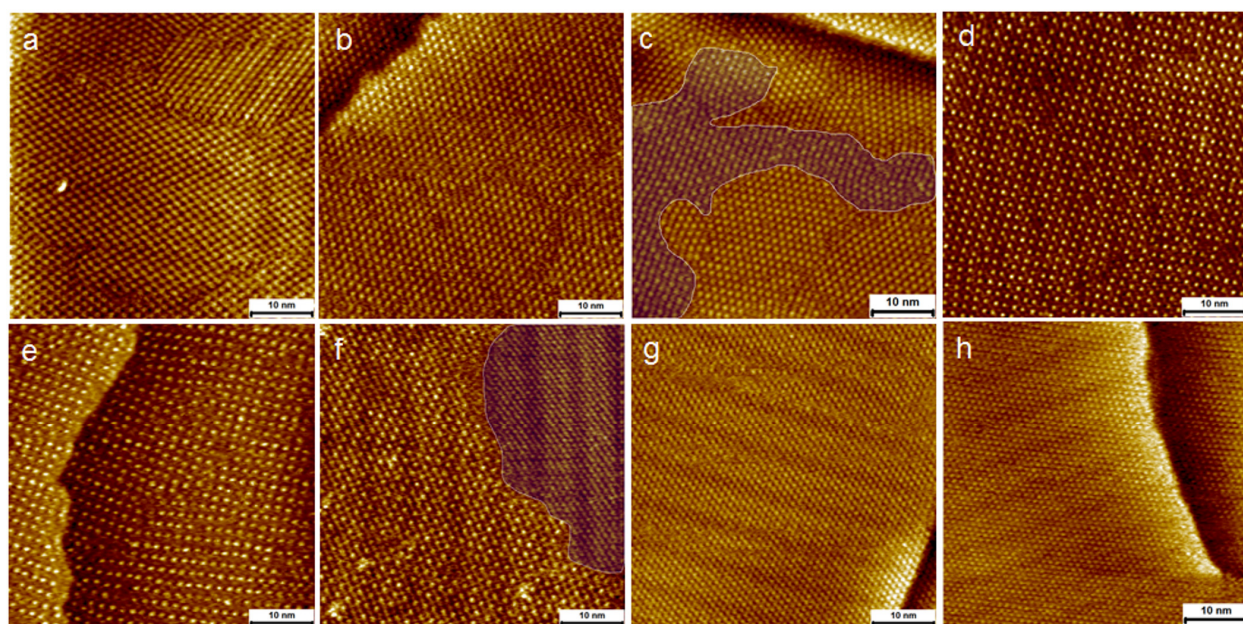
Figure S1. STM images showing different surface structures resulting from adsorption of mixed coronene and CoOEP solutions on clean Au(111) based on different relative molar ratio of coronene:CoOEP, (a) STM image of a sample with 1.8:1 ratio of coronene:CoOEP in solution, surface is covered with only CoOEP structure, (b) STM image of a sample with 18:1 ratio of coronene:CoOEP in solution, surface is covered with only CoOEP structure (c) STM image of a sample with 19:1 ratio of coronene:CoOEP in solution, surface is covered with CoOEP and 1-1 structures, highlighted area is covered with 1-1 structure (d) STM image of a sample with 27:1 ratio of coronene:CoOEP in solution, surface is covered with only 1-1 structure, (e) STM image of a sample with 45:1 ratio of coronene:CoOEP in solution, surface is covered with only 1-1 structure, (f) STM image of a sample with 50:1 ratio of coronene:CoOEP in solution, surface is covered with 1-1 and coronene structures, highlighted area is covered with coronene structure (g) STM image of a sample with 55:1 ratio of coronene:CoOEP in solution, surface is covered with only coronene structure, (h) STM image of a sample with 60:1 ratio of coronene:CoOEP in solution, surface is covered with only coronene structure.

Entrapment of the coronene molecules due to steric hindrance caused by the ethyl substituents of CoOEP: Figure S2 clearly shows that the coronene molecule in 1-1 structure is entrapped by 8 ethyl groups of the neighboring CoOEP molecules.
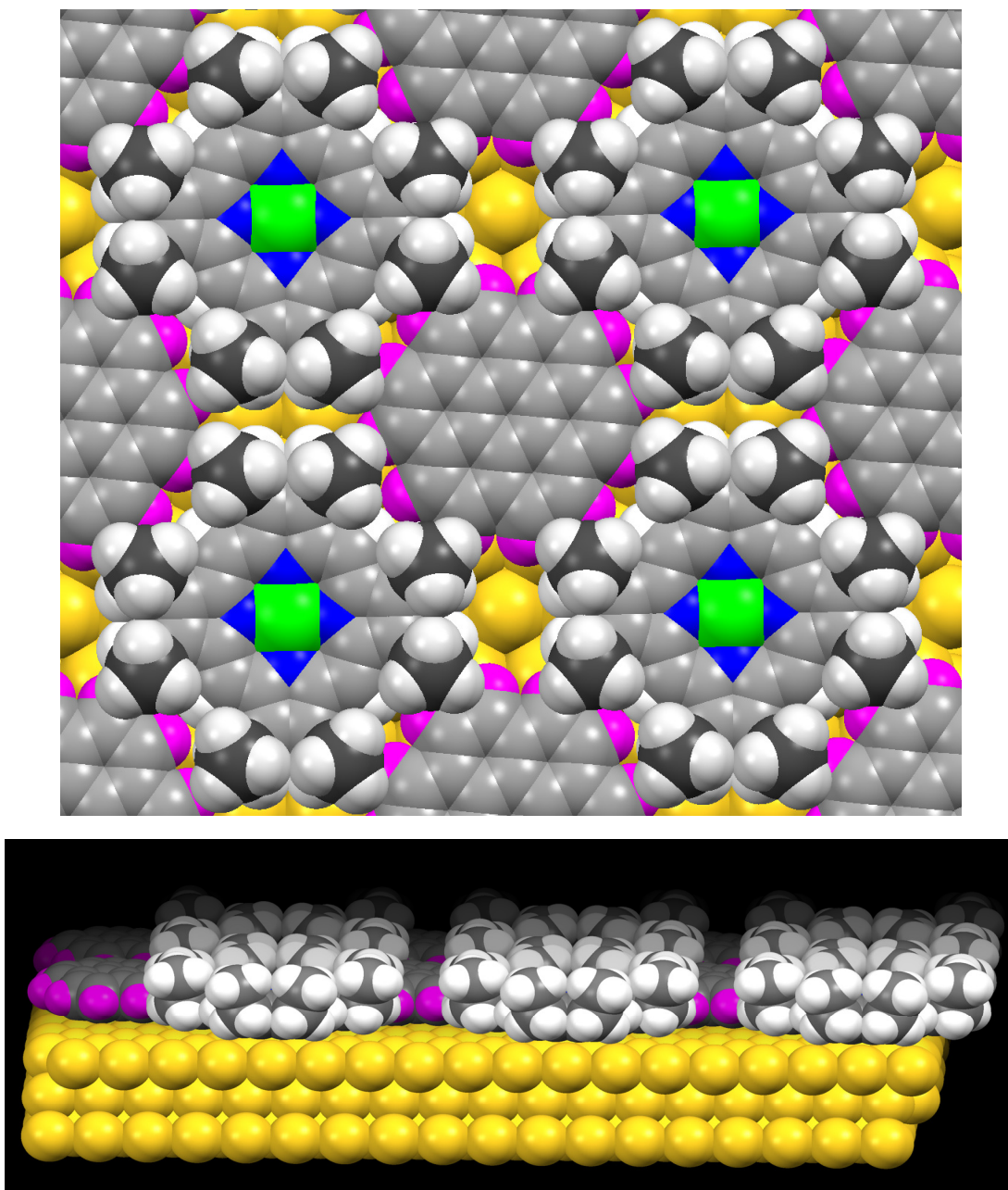

Figure S2. Structure of 1-1 structure composed of one coronene entrapped in the center of unit cell by 4 CoOEP neighboring molecules

Simulation Model:

    To model the interface interactions between the CoOEP and coronene monolayers with Au(111) substrate, appropriate initial geometries are necessary. The guess structures for the simulation were based on current and previously[2,3] obtained experimental data and molecular DFT calculations. A detailed description of how the initial structures were guessed and built is given below.
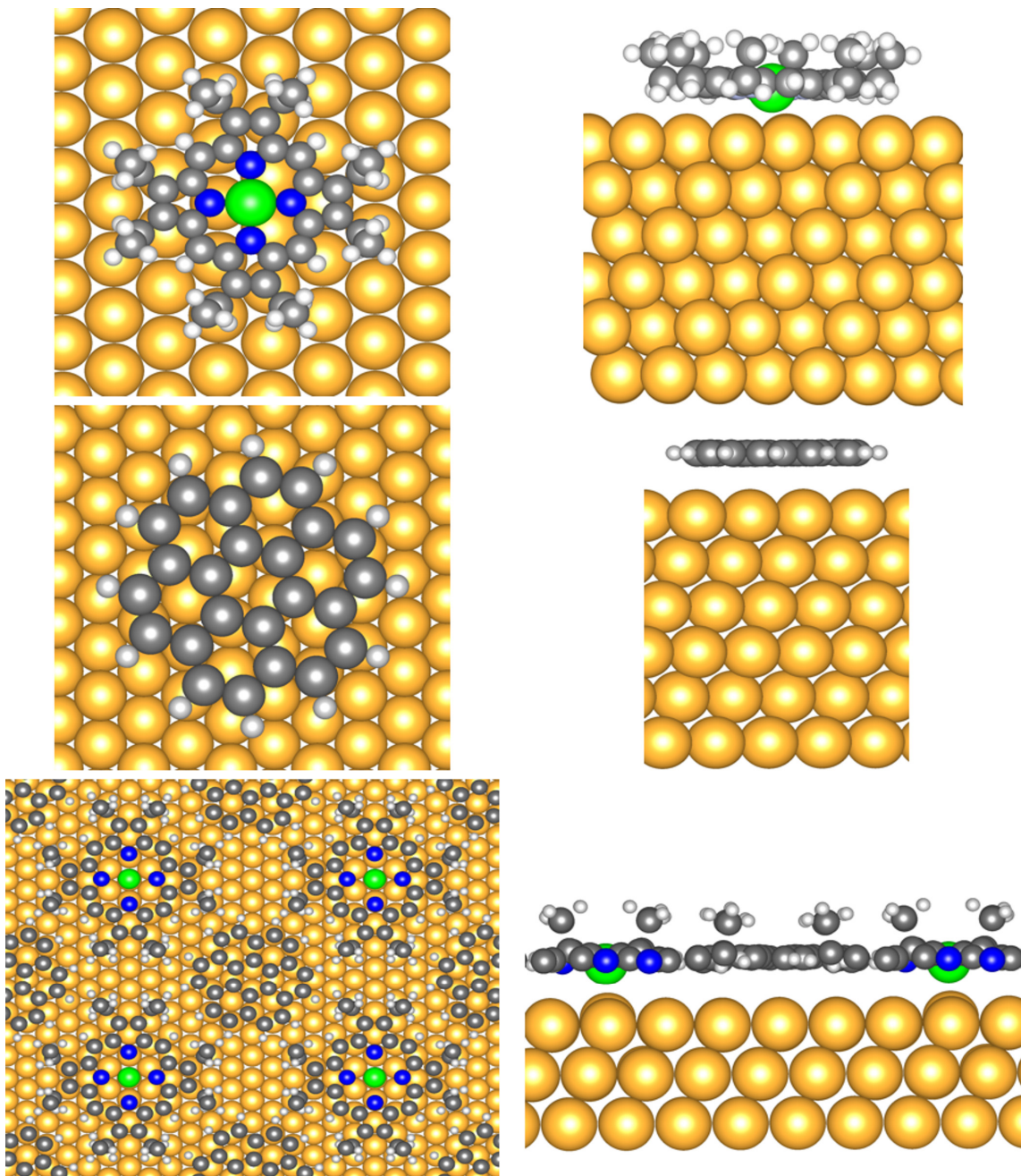
Figure S3. Listed from top to bottom, optimized geometries of CoOEP/Au(111), coronene/Au(111) and CoOEP-Coronene/Au(111) interfaces respectively. Images on the left and right depict the top (along c-axis of unit cell) and side views (along b-axis of unit cell) respectively. Atom colors: Cobalt-green, Carbon-grey, Nitrogen-blue, Hydrogen-white, Gold-yellow.

a) ***Au(111) Surfaces***: Crystal structure unit cell[4] of *fcc*-gold was optimized with plane-wave DFT and were used to build the respective (111) surface. The primary surface of Au(111) were multiplied 6 X 6 X 2, 5 X 5 X 2 in *a, b, c* directions as substrates for CoOEP and coronene systems respectively. In order to build the substrate for 1-1 CoOEP-coronene monolayer, the primary surface of Au(111) was multiplied 8 X 8 X 2 in *a, b, c* directions and then cleaved in the *a, b* directions to match the experimental lattice parameters obtained from STM images (Figure 1). The obtained super cells with lattice parameters listed in Table S1. A vacuum of ~15 Å is added along the c direction for creating a more realistic slab structure for Au(111). Surface reconstruction effects are ignored for all the calculations due to their negligible effects on the monolayer adsorption properties as determined from experimental observations.

b) ***Isolated CoOEP and Coronene Molecules***: Based on the experimental topography of CoOEP[5] and coronene[3] monolayers on Au(111), we generated guess structures for isolated CoOEP and coronene molecules. The CoOEP molecule was built with all the 8 ethyl substituents on the porphyrin stay in an "all up" or "crown" configuration instead of the packing seen in the crystal structure.[6] Similarly, the coronene molecule was built completely flat in the *ab*-plane. Both CoOEP and coronene molecules were optimized using molecular DFT calculations as done previously.[7] The optimized geometries obtained from gas phase molecular calculations were used as the starting geometries for the present study. The lattice parameters for modeling the isolated CoOEP and coronene molecules are listed in Table S1, where the CoOEP and coronene molecules were placed at the center of the cubic box.

Table S1. Lattice parameters of Au(111) slabs, Au(111)/CoOEP, Au(111)/Coronene, Au(111)/CoOEP-Coronene interface systems and isolated CoOEP, Coronene molecules.

System	a (Å)	b (Å)	c (Å)	α (°)	β (°)	γ (°)
Au(111) and Au(111)/CoOEP-Coronene	17.30	15.60	23.14	90	90	90
Au(111) and Au(111)/CoOEP	17.61	17.61	35.38	90	90	120
Au(111) and Au(111)/Coronene	14.42	14.42	30.81	90	90	120
Isolated CoOEP	30	30	30	90	90	90
Isolated Coronene	30	30	30	90	90	90

c) ***CoOEP/Au(111) and Coronene/Au(111) Interfaces***: A single CoOEP and coronene molecules were placed on top of optimized 6 X 6 X 2 and 5 X 5 X 2 slabs of Au(111) respectively, thus transferring the cell parameters of the slabs to the interfaces (Table S1). The proposed slab model with single CoOEP and coronene molecules per unit cell represents a monolayer packing density of ~83% and ~86% respectively on Au(111) under the given substrate parameters (Table S1). Although the exact size of the unit cell of the proposed model differs from experiment, the effect of this difference should be negligible considering weak intermolecular repulsions between hydrogen atoms from neighboring molecules in the observed monolayers of CoOEP[7] and coronene[3] on Au(111) from experiment, which is consistent with our proposed model.

d) ***CoOEP-Coronene/Au(111) Interface***: Form experimental STM images (Figure 1), the 1-1 CoOEP-Coronene monolayer has surface lattice parameters of A = (1.73 ± 0.04) nm, B = (1.56

± 0.04) nm and α = 91˚ ± 2˚. In order to retain the experimental parameters in our simulation, Au(111) slab with lattice parameters (Table 1) that matched with that of experiment (Figure 1) was built. One molecule each of coronene and CoOEP are placed on top of the periodic rectangular Au(111) slab of surface area 17.30×15.60 Å^2. A coronene molecule is placed at the center of the periodic rectangle and one CoOEP molecule is shared at the four corners of the rectangle (Figure 1), thus making it a periodic 1-1 CoOEP-Coronene monolayer. Note that the Au(111) slab used in simulation of CoOEP-Coronene/Au(111) interface has only 3 layers of gold versus 6 layers in both CoOEP/Au(111) and Coronene/Au(111) interface simulations. From our earlier calculations,[8] we found that it is actually the top two layers of Au(111) that actively participate in any kind of geometric changes while bottom 4 would affect very minor to none if at all. Hence our simulated model of CoOEP-Coronene/Au(111) interface is justified as it is and it also helps with speedy simulation even though the surface size is nearly double that of CoOEP/Au(111) and Coronene/Au(111) interface systems.

Calculation of Adsorption Energies:

The adsorption/binding energy of CoOEP, coronene and CoOEP-coronene 1-1 phase on Au(111) substrate can be extracted by subtracting the electronic energies of each respective isolated monolayer and Au(111) substrate from respective monolayer-substrate interface. The equation is as follows:

$$E_{ads} = E_{S-M} - [E_S + E_M]$$

E_{ads} represents the adsorption energy and E_{S-M}, E_S, E_M represents the total energies of individually optimized substrate-monolayer interface, clean substrate and isolated monolayer respectively. All adsorption energies are listed in Table II.

Note that all the energies of adsorption are per unit cell. In case of CoOEP and coronene there is only one molecule per unit cell. So the adsorption energies include molecule-substrate binding energies and intermolecular energies between molecules in the monolayer. But computed intermolecular energies account for only ~2 % to the final adsorption energy while the molecule-substrate binding energies account for ~98%. This can be justified if one considers the proximity of the molecules in the monolayer and type of possible intermolecular forces between them.

Also, note that the calculated unit cell of 1-1 phase structure (built based on experimental STM lattice parameters, Figure 1c, 4) has one molecule each of CoOEP and coronene. From the 1-1 phase structure, three different adsorption quantities were extracted (Table II).

- First the adsorption energy of the entire 1-1 phase monolayer on Au(111).
- Second, the adsorption energy of CoOEP from 1-1 phase monolayer on Au(111). That is energy for removing all of CoOEP molecules from the 1-1 surface while maintaining the coronene molecules in their original position.
- Third, the adsorption energy of coronene from 1-1 phase monolayer on Au(111). That is energy for removing all of coronene molecules from the 1-1 surface while maintaining the CoOEP molecules in their original position.
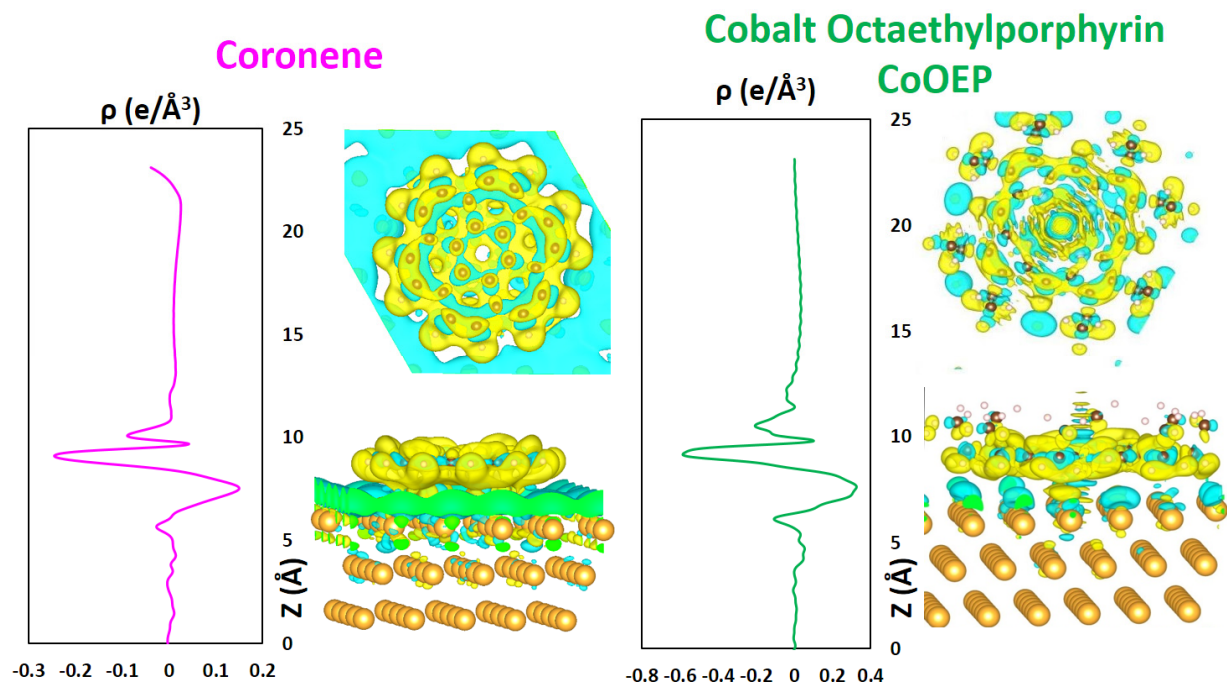
Figure S4. Charge density difference for coronene/Au(111) (left) and CoOEP/Au(111) (right) interfaces. For each image, plot on the left is the x-y plane averaged charge difference, with charge density (ρ) on the x-axis and distance (Å) in z-direction of the interface unit cell on y-axis. Figure on the right represents the 3 dimensional iso-density (+ve: yellow and –ve: cyan) of charge density difference. Note that the charge density difference and pictorial representation of bottom 3 gold layers of the coronene, CoOEP interfaces on Au(111) are masked in the figure or clarity and comparison.
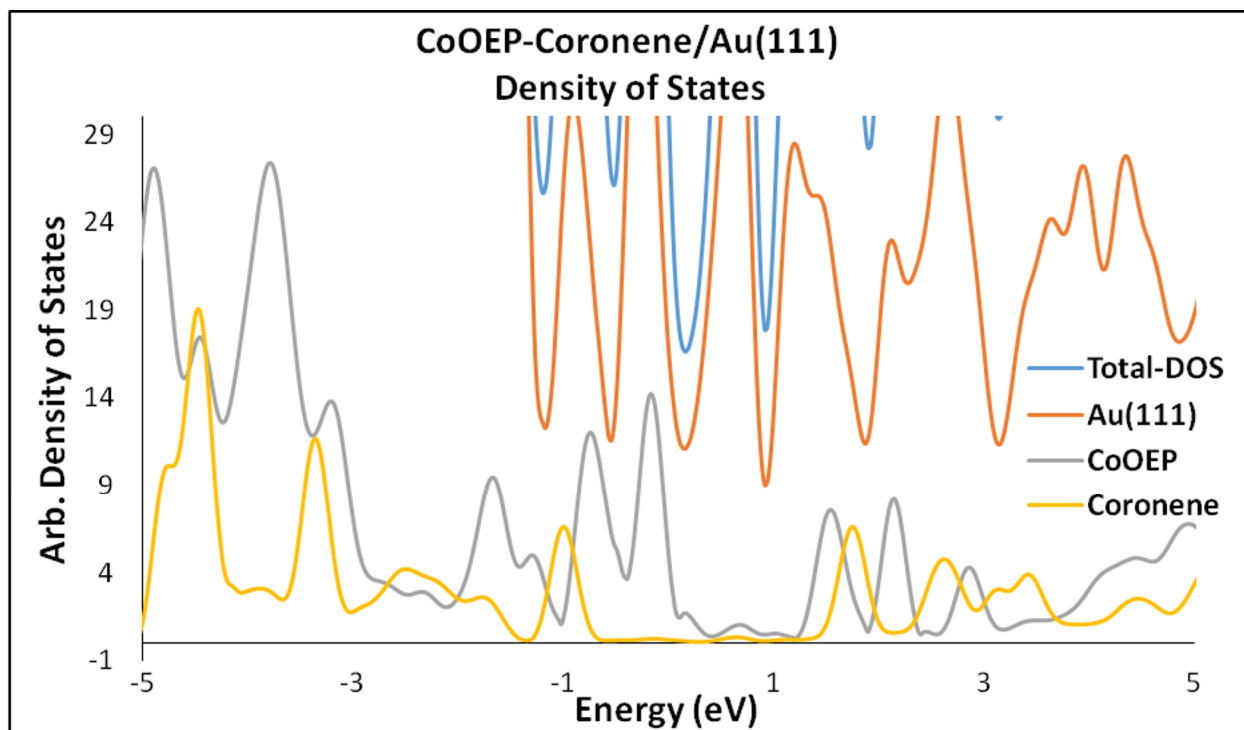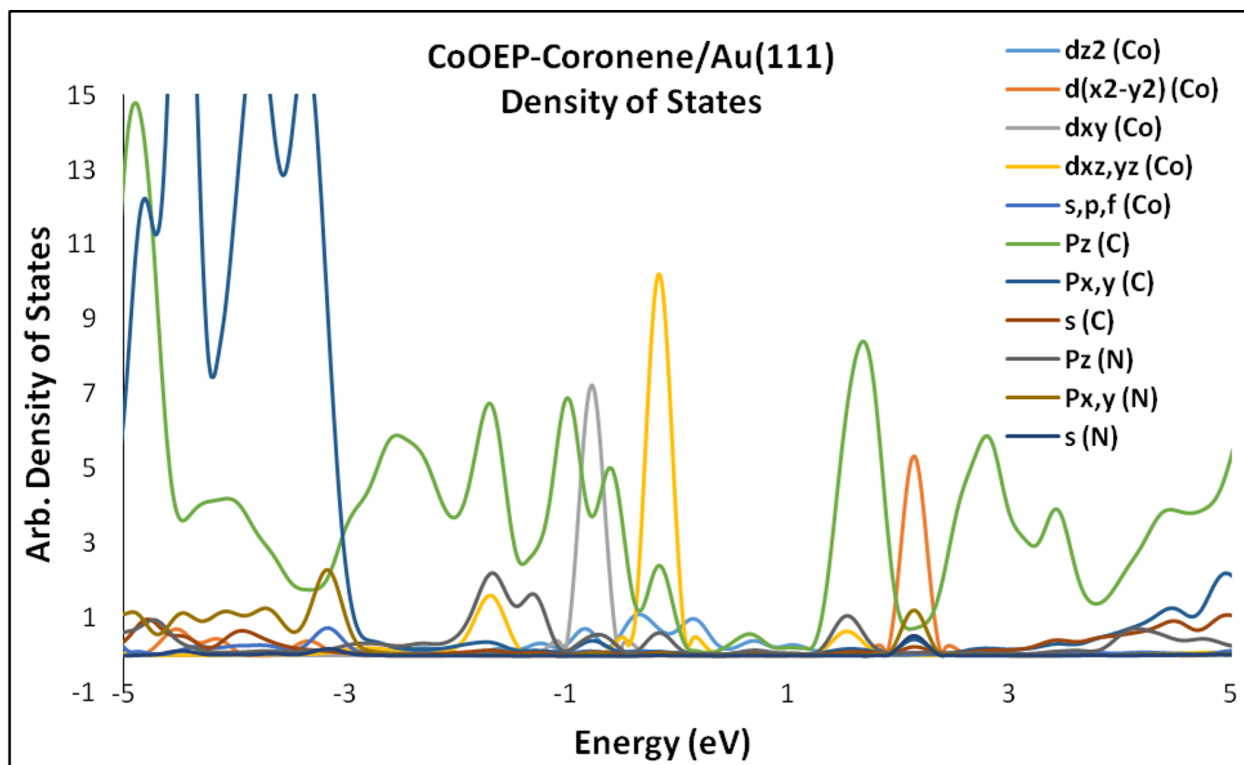
Figure S5. Density of states (DOS) and projected molecule/slab DOS of CoOEP-Coronene/Au(111) interface system. Fermi energy is located at 0 eV.
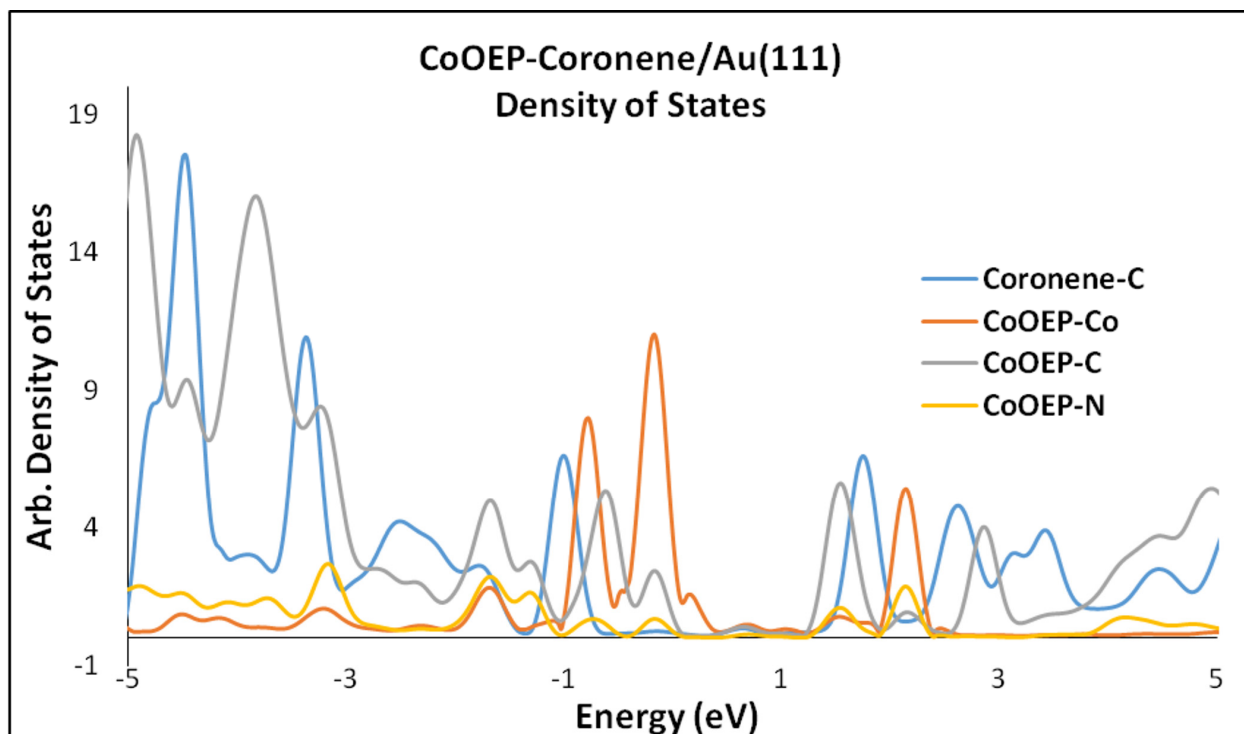
Figure S6. Density of states (DOS) and projected atomic DOS of CoOEP-Coronene/Au(111) interface system. Fermi energy is located at 0 eV.

Figure S7. Projected orbital density of states DOS of CoOEP-Coronene/Au(111) interface system. Fermi energy is located at 0 eV.

Vibrational frequency calculations:

Potential energies of isolated coronene and CoOEP molecules on Au(111) surface were obtained as a function of distance between adsorbate molecule and adsorbent Au(111) surface. The optimized geometries of coronene/Au(111) and CoOEP/Au(111) (*vide supra*) were used to make specific and finite movements of adsorbate molecules to and away from the Au(111) substrate. The respective potential energy surfaces are shown in Figure S8. These energies were they fitted to a polynomial function and the quadratic term was used to calculate a force constant. The harmonic oscillator model and the mass of the appropriate molecule were used to determine a harmonic frequency of vibration.
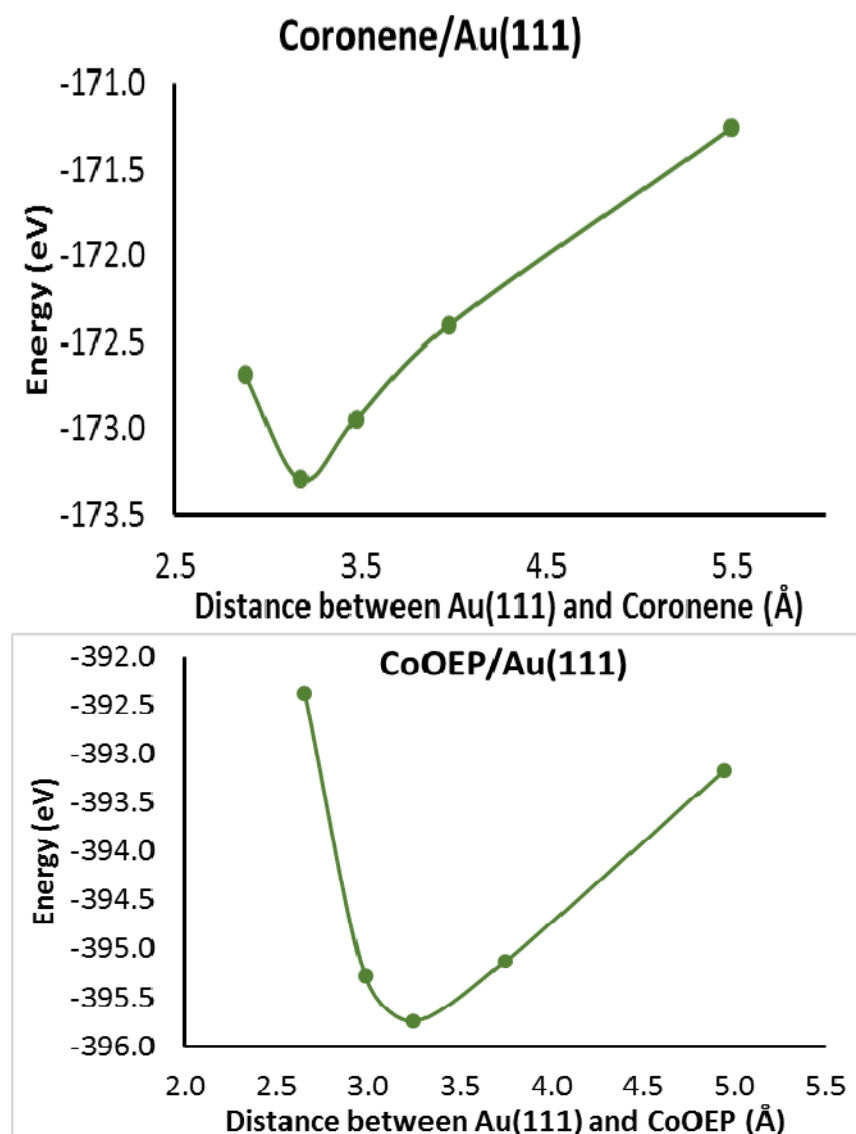
Figure S8: Potential energies of Coronene and CoOEP molecules on Au(111) as function of distance between the molecule and Au(111).

Mechanisms for conversion of 1-1 structure to CoOEP structure: As it mentioned before, for conversion of 1-1 structure to CoOEP structure two mechanisms are possible. In the first mechanism, conversion starts from domain boundaries and it develops through the domain. The other possibility is nucleation of CoOEP structure from inside the domain of 1-1 structure and growth of the structure from there. One example of the first method is indicated in Figure S9. This figure shows the sample at 50 ˚C while 1-1 structure is converting to CoOEP structure. If we compare the area enclosed in the blue box in figures S9(a) and S9(b), (image S9(b) was captured after image S9(a)), we can see that the conversion starts at the upper right hand side of the blue box at the domain boundary of 1-1 structure in figure S9(a). Figure S9(c) shows the happening of the second method. If one focuses attention to the middle of 1-1 structure in the blue box in figure S9(c), nucleation of CoOEP structure can be seen in the middle of the box. Image S9(d) shows the same area after about 30 minutes of capturing image S9(c) which indicates the complete conversion of 1-1 structure to CoOEP structure.
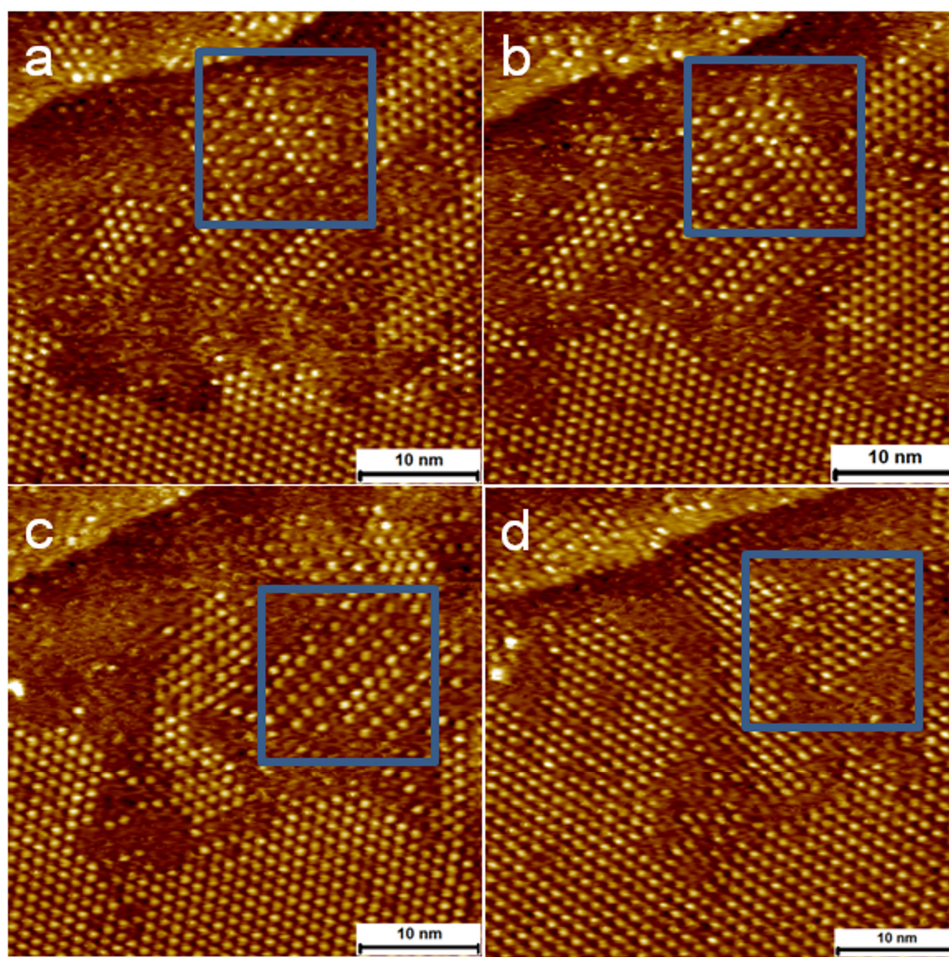

Figure S9. Conversion of 1-1 structure to CoOEP structure at 50 ˚C. Figures (a) and (b) show the possibility of conversion's onset of 1-1 structure to CoOEP structure from domain boundaries. Figure (c) shows the nucleation of CoOEP structure from inside the domain of 1-1 structure. Figure (d) shows the total conversion of 1-1 structure to CoOEP structure.

Measuring Heat of Solution of CoOEP and Coronene in 1-phenyloctane and toluene:

UV-Vis Absorption Spectroscopy was used to measure the heats of solution of CoOEP and coronene in 1-phenyloctane. Heat of solution can be calculated by measuring the solubility of a material in a saturated solution prepared with a specific solvent at different temperatures. Slope of the plot of ln (C) versus 1/T (where C is the saturated concentration and T is the absolute temperature) gives the value of $-\Delta H/R$.[9] We have measured the concentration of saturated solutions of coronene and CoOEP in toluene and 1-phenyloctane at different temperatures. Saturated solutions were stirred well while observable solid compound was present in the solution. Once the temperature became stable, a specific volume of the saturated solution was quickly transferred to a UV-Vis cuvette and the appropriate amount of cold solvent was added to dilute the solution. The concentrations of the saturated solutions were calculated from the absorbance values of the diluted solutions in cuvettes. The temperatures chosen for the solubility measurements include RT, 30, 40, 50 and 60 °C.

Two important points must be noted here in order to accurately perform the experiment. First, the absorbance of diluted solutions should be measurable in the UV-Vis instrument at all temperatures. We kept the absorbance value under 2.0 a.u. to accurately measure the absorbance. Second, the solvent density varies with changing temperature and therefore it might affect the amount of solvent withdrawn at different temperatures. In the temperature range that we performed the experiment density variation was very small.
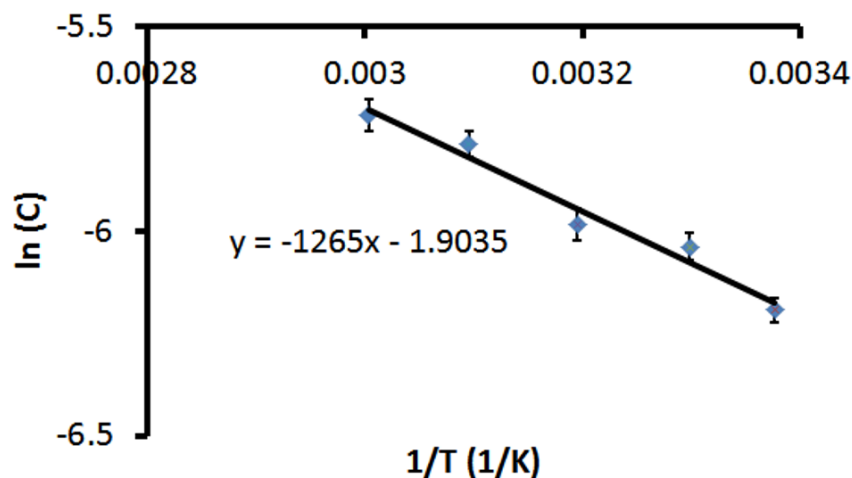
Figure S10: Graph of ln (C) vs. 1/T for Coronene dissolved in 1-Phenyloctane

Table S2. Heat of solution of CoOEP and Coronene in two different solvents

Solute/solvent	Heat of solution (kJ/mol)
CoOEP/1-phenyloctane	17.7 ± 3
coronene/1-phenyloctane	10.5 ± 2

The plot of ln C versus 1/T for coronene in phenyloctane is shown in Figure S10. The results are summarized in table S2.

Energy of desorption in solution versus vacuum:

To good approximation one may write [10]:

$$\Delta E^l = -\Delta E_{sub} + \Delta E + \Delta E_{sol} + \Delta E_{wet} \qquad \text{(eqn 1)}$$

Where ΔE^l is the energy of desorption from gold into phenyloctane, ΔE_{sub} is the energy of sublimation, ΔE is the energy of desorption from gold into UHV, ΔE_{sol} is the energy change when crystalline solid dissolves in phenyloctane, and ΔE_{wet} is the energy associated with the difference in wetting a gold surface and a molecule covered gold surface with phenyloctane.

Because of the nature of the solvent and the absence of voids in the monolayers suitable for solvent co-adsorption, we expect ΔE_{wet} to be small compared to the other terms and will neglect it. In fact, the uncertainties in the individual values likely exceed the wetting term. Table III is a collection of measured, estimated, and calculated values associated with equation 1. Also given in Table III are the resulting estimates for the energy of desorption from gold into phenyloctane and the measured energy of activation for desorption of CoOEP from Au(111) into phenyloctane.

Table S3. Estimated energies for various processes in kJ/mol

Adsorbate	ΔE_{sub} [a]	ΔE_{sol} [b]	ΔE [c,d]	ΔE^l [e]	ΔE_a^l [f]
CoOEP	100 ± 12	18 ± 3	421 (269 ± 25)	339	110 ± 10
coronene	148 ± 10	11 ± 2	233 (124 ± 5)	95	

a) From References [11] and [12]. b) Determined in this study – see supplemental materials. c) From Table II. d) activation energy for desorption from HOPG using reference 13 in parenthesis. e) Assuming that ΔE_{wet} is negligible and using the DFT calculated desorption energy from gold as listed in Table II. f) Value of energy of activation for desorption reported in reference 14.

References

[1] Bhattarai, A.; Mazur, U.; Hipps, K. W. Desorption Kinetics and Activation Energy for Cobalt Octaethylporphyrin from Graphite at the Phenyloctane Solution–Graphite Interface: An STM Study, *J. Phys. Chem. C.*, **2015**, *119* (17), 9386-9394.

[2] Scudiero, L.; Barlow, D. E.; Hipps, K. W. Scanning Tunneling Microscopy, Orbital-Mediated Tunneling Spectroscopy, and Ultraviolet Photoelectron Spectroscopy of Nickel(II) Octaethylporphyrin Deposited from Vapor. *J. Phys. Chem. B* **2002,** *106* (5), 996-1003.

[3] Jahanbekam, A.; Vorpahl, S.; Mazur, U.; Hipps, K. W. Temperature Stability of Three Commensurate Surface Structures of Coronene Adsorbed on Au(111) from Heptanoic Acid in the 0 to 60°C Range. *J. Phys. Chem. C* **2013,** *117* (6), 2914-2919.

[4] Wyckoff; G., R. W. *Crystal Structures*. 2 ed.; Interscience Publishers: New York, New York, 1963; Vol. 1, p 7-83.

[5] Yoshimoto, S.; Inukai, J.; Tada, A.; Abe, T.; Morimoto, T.; Osuka, A.; Furuta, H.; Itaya, K. Adlayer Structure of and Electrochemical O2 Reduction on Cobalt Porphine-Modified and Cobalt Octaethylporphyrin-Modified Au(111) in HClO4. *J. Phys. Chem. B* **2004,** *108* (6), 1948-1954.

[6] Goldberg, D. E.; Thomas, K. M. Crystal and molecular structure of an N-Substituted porphyrin, chloro(2,3,7,8,12,13,17,18-octaethyl-N-ethylacetatoporphine)cobalt(II). *J. Am. Chem. Soc.* **1976,** *98* (4), 913-919.

[7] Friesen, B. A.; Bhattarai, A.; Mazur, U.; Hipps, K. W. Single Molecule Imaging of Oxygenation of Cobalt Octaethylporphyrin at the Solution/Solid Interface: Thermodynamics from Microscopy. *J. Am. Chem. Soc.* **2012,** *134* (36), 14897-14904.

[8] Chilukuri, B.; Mazur, U.; Hipps, K. W. Effect of dispersion on surface interactions of cobalt(ii) octaethylporphyrin monolayer on Au(111) and HOPG(0001) substrates: a comparative first principles study. *Phys. Chem. Chem. Phys.* **2014,** *16* (27), 14096-14107.

[9] Song, W.; Martsinovich, N.; Heckl, W. M.; Lackinger M., Born-Haber cycle for monolayer self-assembly at the liquid-solid interface: Assessing the enthalpic driving force. *J. Am. Chem. Soc.,* **2013**, 135, 14854-14862.

[10] Song, W.; Martsinovich, N.; Heckl, W. M.; Lackinger M., Born-Haber cycle for monolayer self-assembly at the liquid-solid interface: Assessing the enthalpic driving force. *J. Am. Chem. Soc.,* **2013**, 135, 14854-14862.

[11] Edwards, L.; Dolphin, D. Porphyrins: XVI. Vapor absorption spectra and redox reactions: Octalkylporphins. *J. Molec. Spect.* **1970**, *35*, 90-109.

[12] Chickos, J.; Webb, P.; Nichols, G. The enthalpy of vaporization and sublimation of corannulene, coronene, and perylene at T = 298.15 K. *J. Chem. Thermodynamics* **2002**, 34, 1195–1206

[13] Zacharia, R.; Ulbricht, H.; Hertel, T. Interlayer cohesive energy of graphite from thermal desorption of polyaromatic hydrocarbons. *Phys. Rev. B* **2004**, *69*, 155406/1-7.

[14] Bhattarai, A.; Mazur, U.; Hipps, K. W. A single molecule level study of the temperature dependent kinetics for the formation of metal porphyrin monolayers on Au(111) from solution, *J. Am. Chem. Soc.*, **2014**, *136*, 2142−2148